

Internal-state distribution of Na_2^+ produced by associative ionization collisions between $\text{Na}^*(3p)$ atoms

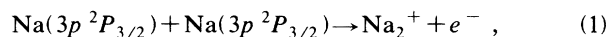
M-X. Wang* and J. Weiner

Department of Chemistry and Biochemistry, University of Maryland, College Park, Maryland 20742

(Received 5 October 1987; revised manuscript received 8 June 1988)

The distribution of internal states in Na_2^+ arising from the associative ionization (AI) collisions, $\text{Na}(3p^2P_{3/2}) + \text{Na}(3p^2P_{3/2}) \rightarrow \text{Na}_2^+ + e^-$, probes the general shape of the potential curves on which the collision takes place. We compare the internal-state distribution extracted from experimental data to those calculated from two sets of recently published potential curves. The results of the comparison indicate that the incoming channels for the AI process follow attractive potentials in the nuclear motion.

Associative ionization (AI) between excited Na atoms,



has become a popular test case for probing the nature of fundamental inelastic collision dynamics. Recent experiments have measured the rate of (1) as a function of velocity for various combinations of electronic angular momentum alignment and orientation.¹⁻⁴ From these measurements and a simple model of angular momentum recoupling,⁵ we have deduced the relative importance of Na_2 molecular-state symmetry classes contributing to process (1).⁶ These experiments and their interpretation, however, provide no clear indication of the general form of the entrance channel potential curves nor of the fundamental bound-free interaction coupling ionizing electrons to the continuum. The experiments described in Refs. 1-4 study the probability of (1) with respect to the *external*-state definition of the colliding partners, i.e., the atomic-state populations prior to collision. Another class of experiments probes the *internal*-state distribution of the product ions either by analysis of the recoil energy in photofragmentation⁷ or by analysis of the energy distribution in the ejected electrons.⁸ The latter technique has enjoyed great success in characterizing both the entrance channel potential curves and the bound-free coupling term in ionizing collisions between metastable rare-gas atoms and various atomic targets. The basic physical picture underpinning the interpretation of these experiments is that Penning and associative ionization are both forms of molecular autoionization in which the final wave function describing the nuclear motion is in a continuum (Penning ionization) or is bound (associative ionization). The nuclear and electronic motions are considered separable (Born-Oppenheimer approximation), and the potential term in the Hamiltonian representing the bound-continuum coupling is complex and local. The real part of this term corresponds to the entrance channel potential curve and the imaginary part is denoted the "resonance width" Γ . The resonance width reflects the loss of scattering probability flux into the final ionizing channel. The local nature of the potential is an approximation based on the tacit recognition that the total-collision en-

ergy between noble-gas metastable atoms and their partners normally lie well above the dissociation limit of the final ionized species. Consequently, all of the bound and many of the continuous product vibrational states are available as exit channels. In the case of process (1) only a few bound vibrational states near the Na_2^+ potential minimum are available, and Lam and George⁹ have challenged the assumption of nonlocality in AI between resonantly excited sodium atoms.

However, the issue of locality versus nonlocality of the interaction can be overcome by applying a theory of free-bound processes developed without recourse to the local approximation. A theory of dissociative recombination (DR), a process related to AI by microreversibility, has been recently presented by Giusti.¹⁰ In the case of weak coupling to the continuum the cross section for AI into a final vibrational level v' may be written

$$\sigma_{\text{AI}}^{v'} = \frac{\pi}{K^2} r \frac{4 |\langle X_{v'}(R) | V(R) | F_d(R) \rangle|^2}{[1 + \pi^2 \sum_v |\langle X_v(R) | V(R) | F_d(R) \rangle|^2]}, \quad (2)$$

where $V(R)$ is the bound-free coupling operator; $X_{v'}(R)$ and $F_d(R)$ the final bound and entrance channel continuum nuclear wave functions, respectively, K the wave vector for the entrance channel, and r a degeneracy factor between initial and final electron states. The sum in the denominator is over all open final vibrational channels. We emphasize that (2) is independent of the local approximation and relies only on the assumption of weak bound-free coupling. Since the cross section for process (1) is known to be small^{11,12} ($\sim 10^{-16}$ cm²) and the probability for ionization estimated to be on the order of 0.1 or less,⁷ application of (2) is appropriate. Although $V(R)$ is a function of the internuclear separation, it is usually slowly varying compared to the oscillations of the nuclear wave functions, $X_{v'}(R)$ and $F_d(R)$; we can replace $V(R)$ by its average \bar{V} . Furthermore, noting that the sum in the denominator is small compared to unity (weak coupling), we write the approximate expression

$$\sigma_{\text{AI}}^{v'} \propto \frac{1}{K^2} |\bar{V}|^2 |\langle X_{v'}^{(R)} | F_d(R) \rangle|^2. \quad (3)$$

Thus we expect the internal-state distribution of the product ion to be governed essentially by Frank-Condon overlap factors between initial and final nuclear wave functions. These factors in turn are sensitive to the shapes of the initial Na_2 molecular potentials along which the collision proceeds. Equation (3) predicts that a manifold of strongly attractive entrance channels will result in a final bound vibrational state distribution contrasting markedly with that arising from a manifold of repulsive states.

In this note we compare Franck-Condon factors generated from two sets of potential curves: one set primarily attractive and adiabatic (see Fig. 1);¹³ the other, repulsive and diabatic with respect to excited Rydberg states of Na_2 ,¹⁴ (see Fig. 2) The distribution of Na_2^+ vibrational levels actually produced in AI collisions, extracted from the photofragmentation spectroscopy of Ref. 7, is then compared to the results of these calculations in order to determine the general form of the potential curves to which the nuclei are subject during the course of the collision.

We calculate the vibrational-level distribution of Na_2^+ from the free-bound Franck-Condon overlaps using the following procedure.

(1) For a given value of collision energy E , we first determine the effective potential for each incoming molecular state of Na_2 and the final state of Na_2^+ in the AI process. The form of the effective potential is given by

$$V_{\text{eff}} = V(R) + Eb^2/R^2, \quad (4)$$

where b is the impact parameter and $V(R)$ the

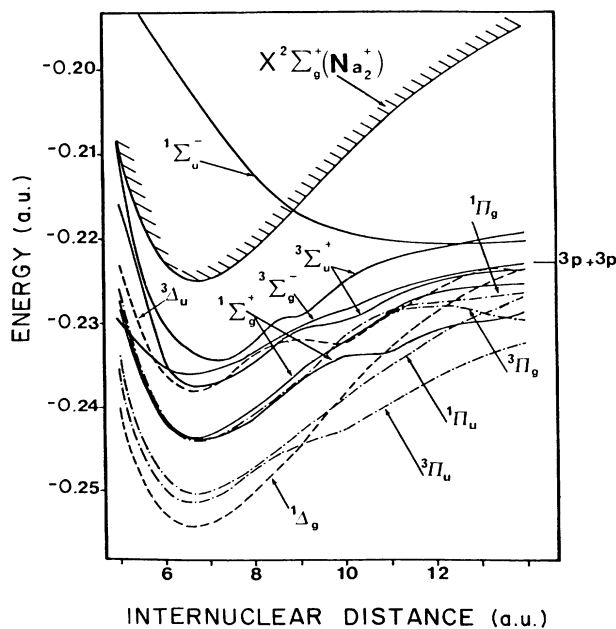


FIG. 1. Attractive molecular curves of $\text{Na}_2(3p+3p)$ taken from Ref. 13.

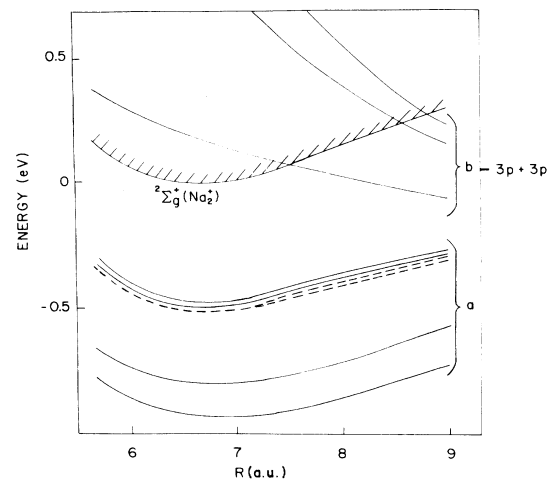


FIG. 2. Repulsive molecular curves of $\text{Na}_2(3p+3p)$ taken from Ref 14.

(electronic-state) potential curve. We average the impact parameter by assuming invariant probability of AI from $b=0$ to b_{max} , with b_{max} set equal to 2 \AA , consistent with the experimental results of Ref. 7.

(2) Having obtained the effective potentials for all the relevant states [using Eq. (4)], we numerically solve the appropriate Schrödinger equations for the eigenvalues and eigenfunctions of nuclear motion $\Psi(E)$ and $\Psi(v')$ of the initial free (Na_2) and the final bound (Na_2^+) states, respectively.

(3) We then calculate all the Franck-Condon overlaps between $\Psi(E)$ and $\Psi(v')$ over the range of collision energies appropriate to the experiment in Ref. 7. We exclude the two Σ states of Na_2 which have negative reflection symmetry $^3\Sigma_g^-$ and $^1\Sigma_u^-$ because an approximate selection rule forbids coupling of these states to the electronic continuum of the $^2\Sigma_g^+$ state of Na_2^+ .

(4) In order to compare a calculated internal-state distribution with experiment, which was carried out in two atomic beams crossed at 180° , we weight the squares of the Franck-Condon factors by the interbeam speed distribution at 700 K. The appropriate relative atomic speed distribution is given by¹⁵

$$\begin{aligned} F(v) &= C^2 \int dv_1 \int dv_2 f(v_1) f(v_2) \delta[v - (v_1 + v_2)] \\ &= C^2 \exp(-mv^2/4kT) \\ &\quad \times \int_0^v dv_2 \exp[-m(v_2 + v/2)^2/kT] (v + v_2)^2 v_2^2, \end{aligned} \quad (5)$$

where $f(v_1)$ and $f(v_2)$ are the Maxwell-Boltzmann speed distributions in each Na beam, v is the relative speed ($v = |\mathbf{v}_1 + \mathbf{v}_2|$), and C is the normalization constant. The relative velocity distribution is calculated and plotted in Fig. 3.

(5) The experimental results of Ref. 7 show that AI produces vibrationally excited Na_2^+ with a fractional popu-

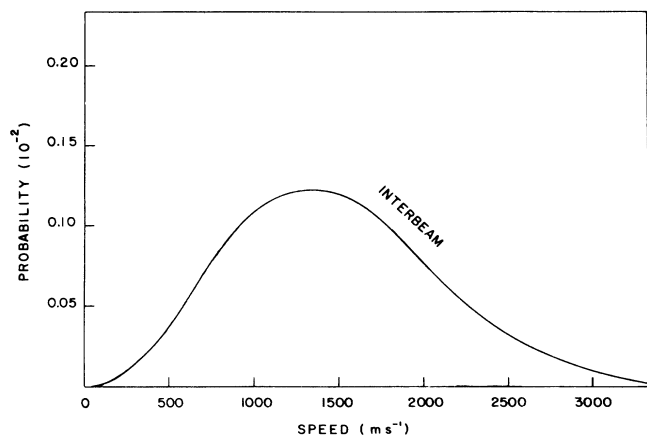


FIG. 3. Interbeam speed distribution, two effusive beams separated by an angle of 180° .

lation distribution increasing approximately linearly with vibrational level. For a given vibrational level v' of the final Na_2^+ electronic term (${}^2\Sigma_g^+$), we sum over the squares of the Franck-Condon factors arising from all possible incoming terms on Na_2 . The summation is weighted according to the statistical degeneracy

$$\begin{aligned} & \frac{1}{32} [3F({}^3\Sigma_u^+(\sigma\sigma)) + F({}^1\Sigma_g^+(\sigma\sigma)) + 3F({}^3\Sigma_u^+(\pi\pi)) \\ & + F({}^1\Sigma_g^+(\pi\pi)) + 6F({}^3\Delta_u) + 2F({}^1\Delta_g) + 2F({}^1\Pi_u) \\ & + 2F({}^1\Pi_g) + 6F({}^3\Pi_u) + 6F({}^3\Pi_g)], \end{aligned} \quad (6)$$

where F designates the square of the Franck-Condon factors corresponding to each incoming term of Na_2 . The calculation is performed for all accessible vibrational levels of Na_2^+ ($v'=0-18$). In Fig. 4 we show the compar-

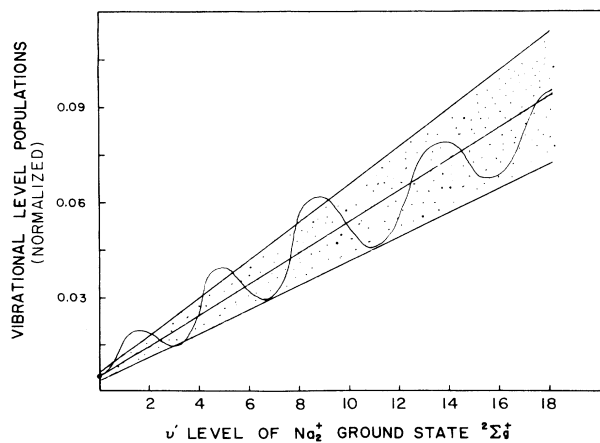


FIG. 4. Distribution of vibrational-level populations of Na_2^+ ground-state ${}^2\Sigma_g^+$ calculated from the attractive states in Fig. 1. The shaded zone represents experimental results of Ref. 7, the curve represents the calculation of the present work.

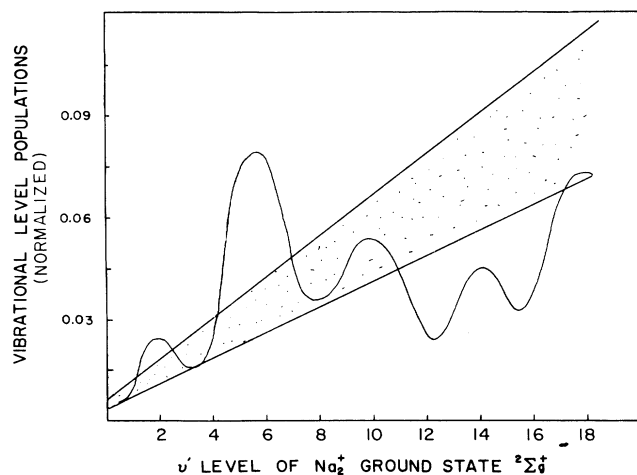


FIG. 5. Distribution of vibrational-level populations of Na_2^+ ground-state ${}^2\Sigma_g^+$, calculated from the b manifold of repulsive states in Fig. 2. The shaded zone represents experiment results of Ref. 7, the curve represents the calculation of the present work.

ison of the calculated fractional vibrational state population, arising from the adiabatic curves of Fig. 1, with the experimental results (the shaded area indicates the limits of experimental uncertainty). It is evident from Fig. 4 that the theoretical distribution derived from the attractive curves fluctuates within a zone increasing with vibrational quantum number, whose slope agrees well with experiment.

Figure 5 compares the same experimental results to a vibrational distribution calculated from the repulsive curves in Fig. 2. The manifold of states labeled "b" in Fig. 2 arise from the strong interaction of singly excited molecular orbital configuration $\sigma_u(3s)\sigma_{u,g}(nl)$, with the doubly excited configuration constructed from $\sigma_g(3p)$, $\sigma_u(3p)$, $\pi_g(3p)$, $\pi_u(3p)$ orbitals. We choose these repulsive diabatic states to carry out the calculations. The results in Fig. 5 clearly show that the Na_2^+ vibrational distribution calculated from the b manifold is at odds with the experimental measurements.

The difference between the two cases stems from the fact that the attractive curves (Fig. 1) produce rapidly fluctuating incoming nuclear continuum wave functions which overlap more effectively with higher-lying functions of Na_2^+ . The repulsive curves (Fig. 2) result in continuum nuclear functions that tend to accumulate around a classical turning point with much less rapid fluctuation, and thus overlap more efficiently with bound functions closer to the Na_2^+ potential minimum. Comparison of calculated and experimental vibrational distributions therefore lends support to the characterization of associative ionization as occurring on essentially attractive pathways.

The work was supported by the National Science Foundation and the University of Maryland Computation Center.

*Present address: Division of Health Science and Technology, Harvard University Medical School, and Massachusetts Institute of Technology, Cambridge, MA 02138.

- ¹M.-X. Wang, J. Keller, J. Boulmer, and J. Weiner, *Phys. Rev. A* **34**, 4497 (1986).
- ²M.-X. Wang, J. Keller, J. Boulmer, and J. Weiner, *Phys. Rev. A* **35**, 934 (1987).
- ³H. A. J. Meijer, H. P. van der Meulen, and R. Morgenstern, *Z. Phys. D* **5**, 299 (1987).
- ⁴H. A. J. Meijer, T. J. C. Pelgrim, H. G. M. Heideman, R. Morgenstern, and N. Anderson, *Phys. Rev. Lett.* **59**, 2939 (1987), and references cited therein.
- ⁵M.-X. Wang, M. S. deVries, and J. Weiner, *Phys. Rev. A* **34**, 1869 (1986).
- ⁶M.-X. Wang and J. Weiner, *Phys. Rev. A* **35**, 4424 (1987).
- ⁷J. Keller, R. Bonanno, M.-X. Wang, M. S. deVries, and J. Weiner, *Phys. Rev. A* **33**, 1612 (1986).
- ⁸An extensive literature on electron energy analysis of Penning and associative ionization has accumulated over the past 20 years. See, for example, J. Lorenzen, H. Hotop, and M.-W. Ruf, *Z. Phys. D* **1**, 261 (1986); J. Lorenzen, H. Morgner, W. Bussert, M.-W. Ruf, and H. Hotop, *Z. Phys. A* **310**, 141 (1983), and references cited therein.
- ⁹K.-S. Lam and T. F. George, *Phys. Rev. A* **32**, 1650 (1985), and references cited therein.
- ¹⁰A. Giusti, *J. Phys. B* **13**, 3867 (1980).
- ¹¹R. Bonanno, J. Boulmer, and J. Weiner, *Phys. Rev. A* **28**, 604 (1983); *Comm. At. Mol. Phys.* **16**, 109 (1985).
- ¹²J. Huennekens and A. Gallagher, *Phys. Rev. A* **27**, 771 (1983).
- ¹³A. Henriët and F. Masnou-Seeuws, *J. Phys. B* **20**, 671 (1987).
- ¹⁴A. Henriët and F. Masnou-Seeuws, in *Abstracts of Contributed Papers, Fifteenth International Conference on the Physics of Electronic and Atomic Collisions, Brighton, 1987*, edited by J. Geddes, H. B. Gilbody, A. E. Kingston, G. J. Latimer, and J. J. R. Walters (Queen's University, Belfast, 1987), p. 716.
- ¹⁵M.-X. Wang, Ph.D. thesis, University of Maryland, 1986.